Journal of Theoretical and Applied Mechanics, Sofia, 2013, vol. 43, No. 4, pp. 49–60

SOLID MECHANICS

ELASTIC PLASTIC PROPERTIES OF MULTIPHASE COMPOSITE BASED ON NON HOMOGENEOUS METAL MATRIX – MODELLING AND SIMULATION*

Ludmila Parashkevova, Nikolina Bontcheva
Institute of Mechanics, Bulgarian Academy of Sciences,
Acad. G. Bonchev St., Bl. 4, 1113 Sofia, Bulgaria,
e-mails: lusy@imbm.bas.bg, bontcheva@imbm.bas.bg

[Received 17 May 2013. Accepted 16 December 2013]

Abstract. A new approach for estimating the mechanical properties of multiphase composite is proposed. The Representative Volume Element (RVE) of the material consists of two different metal matrices and arbitrary number of elastic hardening phases. Multistep homogenization procedures are applied, accounting for influence of the constituent properties, sizes, volume fractions and microstructural distributions. Modified Mori-Tanaka homogenization technique for micropolar media and Budiansky self-consistent method are used for estimation the overall properties of the composite. The theoretical model is applied to description of the properties of precipitation hardening rapidly solidified alloy of the system AlFeVSi with high content of Fe and Si.
Key words: Multiphase composites, Al based alloys, precipitation hardening modelling, micropolar continua.

1. Introduction

The methods of Rapid Solidification (RS) are very effective for obtaining fine and ultra fine microstructure up to nano size leading to higher strengthening, better ductility, fracture toughness and high temperature resistance. These methods allow aluminium based scrap polluted with Fe and Si to be utilized. The manufacturing process consists of two main steps: first step – rapid solidification of melts into thin strips (Fig. 1 and Fig. 2); second step – during which these intermediate products are cut into small pieces, mixed and subjected to cold compaction, preheating and subsequent densification by plastic deformation to form the end product. A so called "in situ" composite is produced during

*Corresponding author e-mail: lusy@imbm.bas.bg

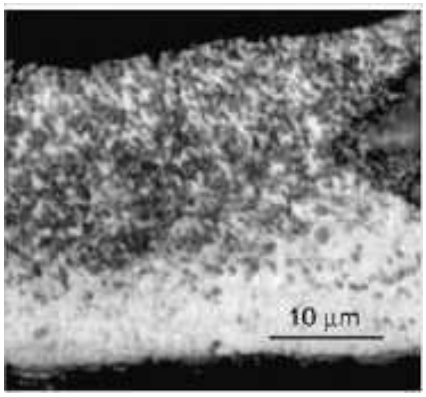

Fig. 1. Microstructure of RS ribbon [1]

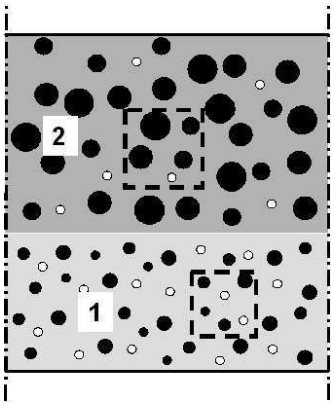

Fig. 2. Scheme of ribbon tailored microstructure

this technological process. The Representative Volume Element (RVE) of such a composite is illustrated in Fig. 3 and Fig. 4. It should be mentioned, that due to cutting and mixing, the final product is heterogeneous but isotropic, in spite of the oriented character of the parent strips. The process of fast cooling leads to formation of two zones. In the zone with higher cooling rate the precipitations are of nano sizes and the volume fraction of intermetallics is higher than the one in the rest of the material. In the second zone with lower cooling rate, precipitations are coarser, of the order of μm, Fig. 1. The mechanical properties of the Al based matrices in both zones are not equal, too. This is a result of the different thermal decomposition conditions in the supersaturated

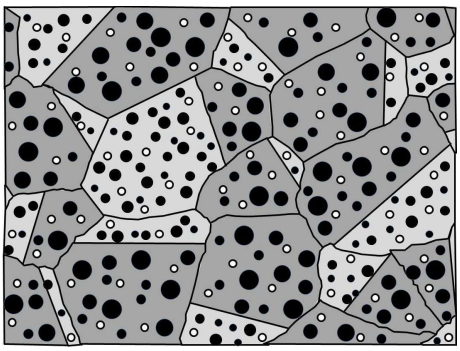

Fig. 3. RVE at micro level before homogenization

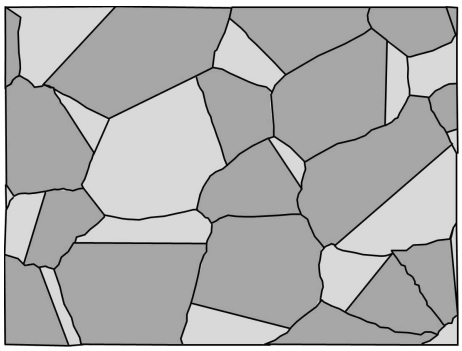

Fig. 4. RVE at micro level after homogenization

matrix. The volume fractions of the phases and the matrix properties in the "in situ" composites depend on the manufacturing conditions unlike the conventionally mixed metal matrix composites. This new "in situ" two metal matrices composite will be modelled and investigated in the present study.

2. Modelling

The approach applied herein consists of multistep homogenization, analogues to the procedure described in [2]. Figures 3 and 4 present schematically RVE of the composite before and after homogenization at micro level, respectively. The ratio between the volume fractions of the dark and the light zones in Fig. 4 corresponds to the ratio of nano and micro size zones of the parent ribbon with cross section illustrated in Fig. 2. The overall properties of the dense end material will be obtained according to the following scheme:

At micro level each of the zones i , $i = 1, 2$ is subjected independently to homogenization. Each zone i is divided into a several number of pseudograins. Each pseudograin is a two-phase composite (matrix and inclusions). The matrix in it depends on the zone i and the inclusions are of a certain size and with certain mechanical properties. The overall properties of each pseudograin are $\overline{K}^{(i)}_{jk}$ and $\overline{G}^{(i)}_{jk}$ The index j stays for the number of hardening phases. In the case considered, we have two such phases: intermetallic precipitations ($j = IM$) and Si ($j = Si$). The index k, $k = 1, \ldots, n^{(i)}_j$ takes into account the different sizes of the corresponding hardening phase. The volume fraction of the hardening phase in each two-phase pseudograin is equal to $C^{(i)}_{sum} = \sum\limits_j C^{(i)}_j = \sum\limits_j \sum\limits_k C^{(i)}_{jk}$, where $C^{(i)}_{jk}$ is the volume fraction of the hardening phase j of size $D^{(i)}_{jk}$ in zone i. The volume fraction of the matrix in it is $C^{(i)}_0 = 1 - C^{(i)}_{sum}$. In what follows the subscript 0 stays for the matrix. The matrix in each zone at micro level is considered as micropolar Cosserat elastic-plastic work-hardening continuum, obeying the relationships given below. The study is restricted to isotropic centro-symmetric micropolar continuum. We assume that the elastic parameters are $E^{(1)}_0 = E^{(2)}_0 = E_0$, $\nu^{(1)}_0 = \nu^{(2)}_0 = \nu_0$ and the Cosserat parameters are $\kappa^{(1)} \neq \kappa^{(2)}$ and the length scale parameters are $l^{(1)}_m \neq l^{(2)}_m$. The intrinsic lengths $l^{(i)2}_m = \alpha^{(i)}/\lambda_0 = \beta^{(i)}/\mu_0 = \gamma^{(i)}/\kappa^{(i)}$ are introduced.

It is assumed that:

$$\kappa^{(1)}/\kappa^{(2)} = \left(l^{(2)}_m/l^{(1)}_m\right)^2, \tag{1}$$

which means that all Cosserat parameters of the matrices are different with exception of the parameters $\gamma^{(1)} = \gamma^{(2)}$. The stress and strain measures are the stress tensor $\sigma_{ij} = \sigma_{(ij)} + \sigma_{\langle ij\rangle}$, the couple stress tensor is $m_{ij} = m_{(ij)} + m_{\langle ij\rangle}$, the strain tensor is $\varepsilon_{ij} = \varepsilon_{(ij)} + \varepsilon_{\langle ij\rangle}$ and the curvature tensor is $k_{ij} = k_{(ij)} + k_{\langle ij\rangle}$. Symbols $(\ldots)$ and $\langle\ldots\rangle$ in the subscript denote the symmetric and antisymmetric parts of a tensor, respectively. The elastic behaviour of the matrix material is described with the well known relations:

$$
\begin{aligned}
&\sigma'_{(ij)} = 2\mu_0\varepsilon'_{(ij)}, \quad \sigma_{\langle ij\rangle} = 2\kappa_0\varepsilon_{\langle ij\rangle}, \quad \sigma_{(kk)} = 3K_0\varepsilon_{(kk)},\\
&K_0 = \lambda_0 + 2\mu_0/3, \quad m'_{(ij)} = 2\beta^{(i)}k'_{(ij)}, \quad m_{\langle ij\rangle} = 2\gamma^{(i)}k_{\langle ij\rangle},\\
&m_{(kk)} = 3N^{(i)}k_{(kk)}, \quad N^{(i)} = \alpha^{(i)} + 2\beta^{(i)}/3,
\end{aligned}
\tag{2}
$$

where λ_0, μ_0 are the elastic Lamé constants, $\alpha^{(i)}$, $\beta^{(i)}$, $\gamma^{(i)}$, $\kappa^{(i)}$ are the Cosserat material constants in zone i. K_0, $N^{(i)}$ are Cauchy and Cosserat bulk modules, respectively. Everywhere in the paper $(\ldots)'$ means deviator. The independent matrix constants in each zone are λ_0, μ_0, $l_m^{(i)}$, $\kappa^{(1)} = \mu_0$ and $\kappa^{(2)}$ is defined with (1).

At the first step, the size sensitive Mori-Tanaka mean field procedure is applied [3] for each pseudograin defined above and the following overall properties are obtained:

$$
\begin{aligned}
&\overline{K}^{(i)}_{jk} = K^{(i)}_0\{1 + C^{(i)}_{sum}(K^{(i)}_{jk} - K^{(i)}_0)/.[C^{(i)}_0 a^{(i)}_0(K^{(i)}_{jk} - K^{(i)}_0) + K^{(i)}_0]\},\\
&\overline{G}^{(i)}_{jk} = G^{(i)}_0\{1 + C^{(i)}_{sum}(G^{(i)}_{jk} - G^{(i)}_0)/.[C^{(i)}_0 b^{(i)}_{0jk}(G^{(i)}_{jk} - G^{(i)}_0) + G^{(i)}_0]\},
\end{aligned}
\tag{3}
$$

where $a^{(i)}_0 = a^{(i)}_0(K^{(i)}_0, G^{(i)}_0)$, $b^{(i)}_{0jk} = b^{(i)}_{0jk}(K^{(i)}_0, G^{(i)}_0, D^{(i)}_{jk}, l^{(i)}_m)$. These properties are obtained following the ideas presented in [4]. After this homogenization step, the material of each pseudograin is Cauchy-type elastic-plastic.

At the second step, the already obtained composites with properties $\overline{K}^{(i)}_{jk}$, $\overline{G}^{(i)}_{jk}$ are further homogenized, finalizing the procedure for each zone i. As all pseudograins have to be treated in a similar way, only symmetric homogenization schemes can be applied. We chose the self-consistent theory for polycrystals. The overall properties $\overline{K}^{(i)}$ and $\overline{G}^{(i)}$ in zone i, depending on the properties of all pseudo grains in it, are solutions of a nonlinear system of equations [2]:

$$
\begin{aligned}
&\sum_{j,k} \frac{\widetilde{C}_{jk}^{(i)}}{1-\dfrac{3\overline{K}^{(i)}}{3\overline{K}^{(i)}+4\overline{G}^{(i)}}\left(1-\dfrac{\overline{K}_{jk}^{(i)}}{\overline{K}^{(i)}}\right)} = 1, \\
&\sum_{j,k} \frac{\widetilde{C}_{jk}^{(i)}}{1-\dfrac{2\left(3\overline{K}^{(i)}+6\overline{G}^{(i)}\right)}{5\left(3\overline{K}^{(i)}+4\overline{G}^{(i)}\right)}\left(1-\dfrac{\overline{G}_{jk}^{(i)}}{\overline{G}^{(i)}}\right)} = 1,
\end{aligned} \tag{4}
$$

where $\widetilde{C}_{jk}^{(i)} = C_{jk}^{(i)} \Big/ C_{sum}^{(i)}$.

At macro level, a third step is realized, homogenizing all zones 1 and all zones 2 to obtain a final overall material. The self-consistent Budiansky method is used [5]. As a result the overall properties $\overline{G}$, $\overline{K}$ (effective shear and bulk modules) are obtained from the following equations system:

$$
\begin{aligned}
&\frac{\widetilde{C}^{(1)}}{1-\dfrac{3\overline{K}}{3\overline{K}+4\overline{G}}\left(1-\dfrac{\overline{K}^{(1)}}{\overline{K}}\right)} + \frac{\widetilde{C}^{(2)}}{1-\dfrac{3\overline{K}}{3\overline{K}+4\overline{G}}\left(1-\dfrac{\overline{K}^{(2)}}{\overline{K}}\right)} = 1\ , \\
&\frac{\widetilde{C}^{(1)}}{1-\dfrac{2\left(3\overline{K}+6\overline{G}\right)}{5\left(3\overline{K}+4\overline{G}\right)}\left(1-\dfrac{\overline{G}^{(1)}}{\overline{G}}\right)} + \frac{\widetilde{C}^{(2)}}{1-\dfrac{2\left(3\overline{K}+6\overline{G}\right)}{5\left(3\overline{K}+4\overline{G}\right)}\left(1-\dfrac{\overline{G}^{(2)}}{\overline{G}}\right)} = 1,
\end{aligned} \tag{5}
$$

where $\widetilde{C}^{(i)}$ are the volume fractions of all zones of type (i) in the macro RVE, see Fig. 4.

Let Ω, V_{IM} denote the entire volume and the intermetallic phase volume in a unit length of the ribbon; Ω_i, $V_{IM}^{(i)}$, $C_{IM}^{(i)}$, $d_{IM}^{(i)}$ are volumes, phase volumes, volume fraction and precipitation size of intermetallics in zone i, $i = 1, 2$. We assume $\Omega_1 = k_{WS}\Omega$, $0 < k_{WS} < 1$. The parameter k_{WS} determines the volume of the "nano" zone of high cooling rate. The thickness of this zone strongly depends on the tangential velocity of the cooling wheel during ribbon formation. Experiments show that higher velocity leads to thinner but harder nano zone with higher precipitations volume fraction. Let $V_{Si}^{(i)}$ and $d_{Si}^{(i)}$ be the volume and precipitation size of Si in zone i, $i = 1, 2$. The total volume fraction of

precipitated intermetallic is $V_{IM}/\Omega = \left(V_{IM}^{(1)} + V_{IM}^{(2)}\right)/\Omega = P = \text{const}$, and the volume fraction of Si precipitations is $V_{Si}/\Omega = \left(V_{Si}^{(1)} + V_{Si}^{(2)}\right)/\Omega = S = \text{const}$, both depending on the chemical composition of the alloy. The parameters P and k_{WS} are related with:

$$P = k_{WS}\frac{V_{IM}^{(1)}}{\Omega_1} + (1 - k_{WS})\,\frac{V_{IM}^{(2)}}{\Omega_2} = k_{WS}C_{IM}^{(1)} + (1 - k_{WS})\,C_{IM}^{(2)}, \tag{6}$$

and the following limits hold:

$$k_{WS} \to 0 \quad C_{IM}^{(2)} \to P, \quad k_{WS} \to 1 \quad C_{IM}^{(1)} \to P. \tag{7}$$

It is assumed that $C_{IM}^{(1)}\Big|_{k_{WS}\to 0} = \max C_{IM}^{(1)} = C_{per}$, and if $C_{IM}^{(2)}\Big|_{k_{WS}\to 1} \to C_{IM}^{(1)}\Big|_{k_{WS}\to 1}$, then $C_{IM}^{(2)}\Big|_{k_{WS}\to 1} = P$.

As we are dealing with approximately spherical inclusions, the maximal volume fraction of intermetallic precipitations is restricted by the percolation limit $C_{per} = 0.63$ [6].

Experiments show, that the volume fractions of the Si phase $C_{Si}^{(i)}$ are approximately the same in both zones.

We denote $C_{IM}^{(1)}/C_{IM}^{(2)} = q\,(k_{WS})$ where $C_{IM}^{(i)} = V_{IM}^{(i)}/\Omega_i$, $i = 1, 2$. On the base of analysis of microhardness measurements provided at both sides of ribbon specimens, the following form of $q\,(k_{WS})$ is suggested:

$$q\,(k_{WS}) = 1 + \left(\frac{C_{per}}{P} - 1\right)(1 - k_{WS})^{\beta_{IM}}, \tag{8}$$

where $\beta_{IM} > 1$ is correlated to the experimental data (see Fig. 5). This is a further development of the ideas for the case $q\,(k_{WS}) = 1$, presented in [2]. The form of the curve described by (8) corresponds qualitatively to the curve defined by the experimental points of hardness at both zones, shown in Fig. 5.

At given P and k_{WS} the intermetallic volume fractions are:

$$C_{IM}^{(2)} = \frac{P}{q\,(k_{WS})\,k_{WS} - k_{WS} + 1}, \quad C_{IM}^{(1)} = q\,(k_{WS})\,C_{IM}^{(2)}. \tag{9}$$

The elastic state of the already homogenized composite material is now described by the overall characteristics $\overline{K}$ and $\overline{G}$.

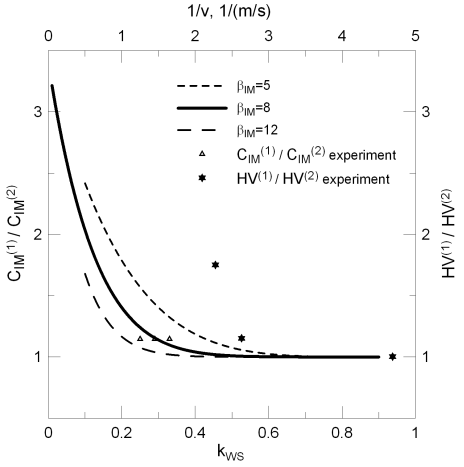

Fig. 5. Influence of nano zone size on intermetallic relative volume fraction

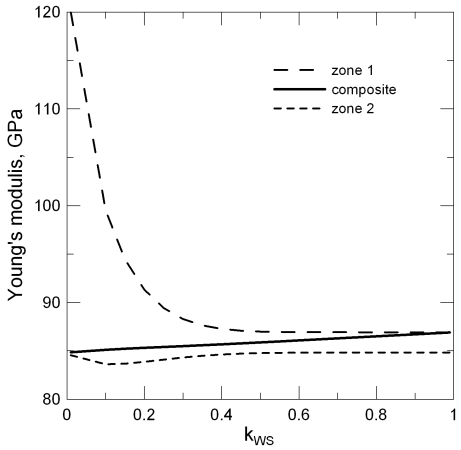

Fig. 6. Elastic properties depending on the nano size zone volume fraction

The plastic properties of the composite on macro level are based on the plastic properties of the Al matrices. It is assumed that both matrices obey one and the same plastic strain hardening law $\sigma_{pAl} = \sigma_{0Al} + h_0 \left(\overline{\varepsilon}_p\right)^{n_0}$. σ_{0Al} is the initial yield stress, h_0 and n_0 are hardening parameters, $\overline{\varepsilon}_p$ is the accumulated equivalent plastic strain.

Following the approach in [4], we obtain the initial yield stress of the composite material in each zone $\sigma_{p0}^{(i)}$, $i = 1, 2$. Each of this yield limits depends on the corresponding matrix material and volume fraction and sizes of hardening precipitations.

Denote $\sigma_{pm} = \min\left(\sigma_{p0}^{(1)}, \sigma_{p0}^{(2)}\right)$, which determines $m = 1$ or $m = 2$, depending on the fact, which is the softer zone. We assume that plastic state of the overall composite takes place when the volume averaged equivalent stress in the domain $\overline{\Omega}_m$, formed by all zones of type m reaches the limit σ_{pm}, i.e.:

$$\left\langle \overline{\sigma}_e^2 \right\rangle_{(m)} = \sigma_{pm}^2, \tag{10}$$

where $\overline{\sigma}_e$ is the equivalent von Mises stress.

In the frame of RVE (Fig. 4) of the composite, we consider the already yielded domain $\overline{\Omega}_m$ as a plastic matrix and the rest of RVE as a dispersed still elastic phase. Hill's strain energy equivalent condition is adopted and is used to estimate the averaged equivalent stress appearing in the yield condition (10). As after the homogenization, the end material is isotropic of Cauchy type, the

strain energy is:

$$\langle \sigma_{ij}\varepsilon_{ij}\rangle_{RVE} = \Sigma_{ij}E_{ij} = \frac{1}{2\overline{G}}\Sigma'_{ij}\Sigma'_{ij} + \frac{1}{9\overline{K}}\Sigma^2_{kk}. \tag{11}$$

We apply the variation technique given in [7], simplified for Cauchy material. This means that only the modulus $\overline{G}^{(m)}$ is varied. Thus using (11) we obtain

$$\widetilde{C}^{(m)}\frac{\partial}{\partial\overline{G}^{(m)}}\left\langle\frac{1}{2\overline{G}^{(m)}}\sigma'_{ij}\sigma'_{ij} + \frac{1}{9\overline{K}^{(m)}}\sigma^2_{kk}\right\rangle_{\overline{\Omega}_m} = \frac{\partial}{\partial\overline{G}^{(m)}}\left(\frac{1}{2\overline{G}}\Sigma'_{ij}\Sigma'_{ij} + \frac{1}{9\overline{K}}\Sigma^2_{kk}\right). \tag{12}$$

It is taken into account in (12) that the material properties in the still elastic zone do not depend on $\overline{G}^{(m)}$.

As far as $\partial\overline{K}^{(m)}/\partial\overline{G}^{(m)} = 0$, the needed averaged equivalent stress is given with:

$$\left\langle\frac{3}{2}\sigma'_{ij}\sigma'_{ij}\right\rangle_{\overline{\Omega}_m} = \frac{1}{\widetilde{C}^{(m)}}\left[\frac{3}{2}\frac{\overline{G}^{(m)2}}{\overline{G}^2}\frac{\partial\overline{G}}{\partial\overline{G}^{(m)}}\Sigma'_{ij}\Sigma'_{ij} + \frac{1}{3}\frac{\overline{G}^{(m)2}}{\overline{K}^2}\frac{\partial\overline{K}}{\partial\overline{G}^{(m)}}\Sigma^2_{kk}\right]. \tag{13}$$

The yield condition of the final composite written in the traditional form states:

$$\frac{3}{2}\Sigma'_{ij}\Sigma'_{ij} + \frac{A^2}{9B^2}\Sigma^2_{kk} - \sigma^2_{pc} = 0, \tag{14}$$

where $\dfrac{1}{A^2} = \dfrac{1}{\widetilde{C}^{(m)}}\dfrac{\overline{G}^{(m)2}}{\overline{G}^2}\dfrac{\partial\overline{G}}{\partial\overline{G}^{(m)}}$, $\dfrac{1}{9B^2} = \dfrac{1}{3\widetilde{C}^{(m)}}\dfrac{\overline{G}^{(m)2}}{\overline{K}^2}\dfrac{\partial\overline{K}}{\partial\overline{G}^{(m)}}$.

The initial yield stress of the composite is:

$$\sigma_{pc} = A\sigma_{pm}, \tag{15}$$

where $\sigma_{pm} = A_c^{(m)}\sigma_{0Al}$, and

$$\frac{1}{A_c^{(m)2}} = \frac{1}{C_0^{(m)}}\left(\frac{G_0^{(m)2}}{\overline{G}^{(m)2}}\frac{\partial\overline{G}^{(m)}}{\partial G_0^{(m)}} + \frac{\beta^{(m)2}}{l_m^{(m)2}\overline{G}^{(m)2}}\frac{\partial\overline{G}^{(m)}}{\partial\beta^{(m)}} + \frac{\gamma^{(m)2}}{l_m^{(m)2}\overline{G}^{(m)2}}\frac{\partial\overline{G}^{(m)}}{\partial\gamma^{(m)}}\right).$$

No matter that the matrices are of von Mises yielding type, the yield condition of the composite (14) in general depends on the first stress invariant at macro level. Thus, the existence of inclusions as constituents of the composite material is taken into account in some averaged manner. It is shown in [4], that the yield condition of the composite does not depend on the first stress invariant and coincides with the von Mises yield condition only if the bulk modules of all constituents are equal. In the case of naturally arisen "in situ" composite such an equality assumption for the bulk modules is feasible as up to rather high degrees of plastic deformation no debonding has been experimentally observed.

3. Numerical simulation

The modelling presented is applied to a composite material obtained after RS of AlFe9V2Si7 alloy followed by cutting, mixing, compacting and preheating [1]. All mechanical and physical properties needed for the modelling are given in Table 1. The intrinsic parameters $l_m^{(i)}$ correspond to the grain sizes of the Al matrices in each zone, which are experimentally observed. The function $q\,(k_{WS})$ is illustrated in Fig. 5 for different values of the parameter β_{IM}. Experimental measurements on chemical elements analysis of ribbon surfaces provided in [1] estimate that in the interval $0.25 \leq k_{WS} \leq 0.33$, $C_{IM}^{(1)}/C_{IM}^{(2)} = 1.143$. According to this, we choose $\beta_{IM} = 8$. The curve, describing the variation of the experimental relative hardness $HV^{(1)}/HV^{(2)}$ of both zones with the cooling wheel velocity v is also shown in Fig. 5. It is proved experimentally [8], that the width of the nano size zone is inversely proportional to the cooling wheel velocity. On the other hand, the amount of hardening precipitations influences the hardness. The proper choice of the mathematical expression for $q\,(k_{WS})$ with parameter β_{IM} ensures the required similarity of both curves, given in Fig. 5.

The plastic properties of both matrices are: $\sigma_{0Al} = 122$ MPa, $h_0 = 173$ MPa and $n = 0.455$.

The aim of the numerical simulation is to investigate the influence of the ultrafine zone 1 with higher volume fraction of intermetallic precipitations, depending on the parameters k_{WS}. The latter is correlated to technological parameters like wheel angular velocity, melt temperature, the total strip thickness etc. The change of the elastic properties of the overall composite is shown in Fig. 6 for the case of precipitations sizes in zone 2 for intermetallic $d_{IM}^{(2)} = 0.3$ μm and for Si $d_{Si}^{(2)} = 0.24$ μm. A small increase of the initial yield limit of the

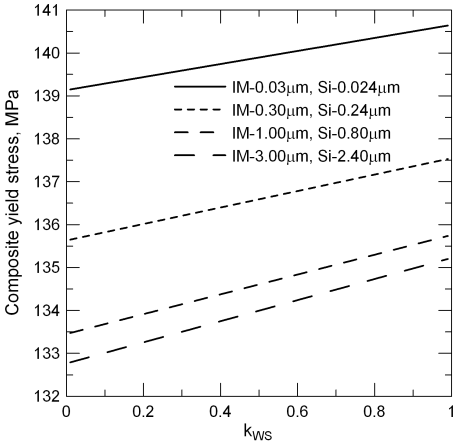

Fig. 7. Composite yield stress at different values of $d_{IM}^{(2)}$ and $d_{Si}^{(2)}$

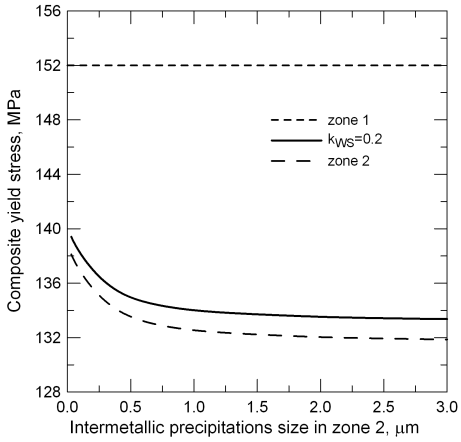

Fig. 8. Size sensitivity of the composite yield stress

Table 1. Material parameters

Properties	Matrix		Intermetallic		Si	
	Zone 1	Zone 2	Zone 1	Zone 2	Zone 1	Zone 2
Young's modulus, GPa	71.0	71.0	156.2	156.2	110.0	110.0
Poisson's ratio	0.34	0.34	0.148	0.148	0.25	0.25
$l_m^{(i)}$, μm	0.04	0.07	–	–	–	–
κ_0, GPa	53.0	17.31	–	–	–	–
Precipitation size, μm	–	–	0.01	0.03–3.0	0.008	0.024–2.4

composite compared to the one of the zone 2 verifies the leading role of the softer zone on the transition of the material from elastic to plastic state. The numerical simulation provided shows almost linear dependence of the Young's modulus on the volume fraction of the nano size zone 1. The size sensitivity of the yield limit depending on the nano zone width is seen in Fig. 7. It is seen, that the dependence on k_{WS} is almost linear. With decreasing the precipitations size, the composite initial yield stress increases but the character of the dependence on k_{WS} remains linear, with the same slope. The yield limits of the materials in both zones are plotted in Fig. 8. As far as the yield limit is correlated linearly to hardness, the numerical results are in accordance with the microhardness, measured at both sides of the parent ribbon made of AlFe9V2Si7 alloy, provided in [1]. These experimental observations show that

with increasing the cooling rate, corresponding to lower values of k_{WS}, the microhardness at the nano size zone 1 becomes much higher than the one in the micro size zone 2. The results of numerical simulations, illustrated in Fig. 8 show that the yielding of the overall composite is controlled by the yielding of the softer zone.

The calculations, illustrated in Figs 6, 7 and 8 are performed for $d_{IM}^{(1)} = 0.01$ μm and $d_{Si}^{(1)} = 0.008$ μm, which correspond to the values experimentally obtained on the wheel side of the ribbons.

4. Conclusions

The model presented describes the material behaviour of a metal matrix based composite, hardened by multiphase precipitations. The numerical simulations show that the increase of the cooling wheel velocity has no significant influence on the overall properties of the material. High cooling velocity leads to a zone of much harder material but very thin. The improvement of certain mechanical properties in this zone takes place simultaneously with some deteriorations of those properties in the rest part of the parent ribbon. These properties variations are inherited by the "in situ" composite considered.

REFERENCES

[1] Yaneva, S., N. Stoichev, G. Avdeev, R. Petrov, A. Davidkov. Development of Nanozones in Microcrystalline Alloys based on the Al-Fe-V-Si System. *Metallurgist*, **54** (2010), 459–467.

[2] Parashkevova, L., N. Bontcheva. Strengthening of Multiphase Al based Composites. *Comptes rendus de l'Académie bulgare des Sciences*, **66** (2013), No. 8, 1175–1182.

[3] Hu, G., X. Liu, T. J. Lu. A Variational Method for Non-linear Micropolar Composites. *Mechanics of Materials*, **37** (2005), 407–425.

[4] Parashkevova, L., N. Bontcheva, V. Babakov. Modelling of Size Effects on Strengthening of Multiphase Al based Composites. *Comput. Mater. Sci.*, **50** (2010), No. 2, 527–537.

[5] Budiansky, B. On the Elastic Moduli of Some Heterogeneous Materials. *J. Mech. Phys. Solids*, **13** (1965), 223–227.

[6] Privalko, V. P., V. F. Shumsky, E. G. Privalko, V. M. Karaman, R. Walter, K. Friedrich, M. Q. Zhang, M. Z. Rong. Viscoelasticity and Flow Behaviour of Irradiation Grafted Nano-inorganic Particle filled Polypropylene Composites in the Melt State. *J. Mater. Process. Technol.*, **137** (2003), 208–213.

[7] Parashkevova, L., N. Bontcheva. Influence of Precipitations on Elastic-plastic Properties of Al Alloys. *Comput. Mater. Sci.*, **47** (2009), 153–161.

[8] Jurci, P., M. Hudakova, M. Domankova, B. Sustarsic, J. Serak. Microstructure and Properties of Binary Al7Cr Alloy prepared by Rapid Solidification, In: Proc. METAL 2008 – 17th International Metallurgical & Material Conference, Czech Republic, Hradec nad Moravicí, May 13–15 2008, CD-ROM – 038.